



HAL
open science

Exact Modal Methods

Boris Gralak

► **To cite this version:**

Boris Gralak. Exact Modal Methods. E. Popov. Gratings: Theory and Numeric Applications, AMU (PUP), pp.10.1-10.21, 2012, 978-2-8539-9860-4. hal-00785120

HAL Id: hal-00785120

<https://hal.science/hal-00785120>

Submitted on 5 Feb 2013

HAL is a multi-disciplinary open access archive for the deposit and dissemination of scientific research documents, whether they are published or not. The documents may come from teaching and research institutions in France or abroad, or from public or private research centers.

L'archive ouverte pluridisciplinaire **HAL**, est destinée au dépôt et à la diffusion de documents scientifiques de niveau recherche, publiés ou non, émanant des établissements d'enseignement et de recherche français ou étrangers, des laboratoires publics ou privés.

GRATINGS: THEORY AND NUMERIC APPLICATIONS

Tryfon Antonakakis
Fadi Baïda
Abderrahmane Belkhir
Kirill Cherednichenko
Shane Cooper
Richard Craster
Guillaume Demesy
John DeSanto
G rard Granet

Boris Gralak
S bastien Guenneau
Daniel Maystre
Andr  Nicolet
Brian Stout
Fr d ric Zolla
Benjamin Vial

Evgeny Popov, Editor

Institut Fresnel, Universit  d'Aix-Marseille, Marseille, France
Femto, Universit  de Franche-Comt , Besan on, France
Institut Pascal, Universit  Blaise Pascal, Clermont-Ferrand, France
Colorado School of Mines, Golden, USA
CERN, Geneva, Switzerland
Imperial College London, UK
Cardiff University, Cardiff, UK
Universit  Mouloud Mammeri, Tizi-Ouzou, Algeria

ISBN: 2-85399-860-4

www.fresnel.fr/numerical-grating-book

ISBN: 2-85399-860-4

First Edition, 2012, Presses universitaires de Provence (PUP)

World Wide Web:

www.fresnel.fr/numerical-grating-book

Institut Fresnel, Université d'Aix-Marseille, CNRS
Faculté Saint Jérôme,
13397 Marseille Cedex 20,
France

Gratings: Theory and Numeric Applications, Evgeny Popov, editor (Institut Fresnel, CNRS, AMU, 2012)

Copyright © 2012 by Institut Fresnel, CNRS, Université d'Aix-Marseille, All Rights Reserved

Chapter 10:
Exact Modal Methods

Boris Galak

Table of Contents:

10.1	Introduction	1
10.2	Notations	2
10.3	Continuation of the electromagnetic field	4
10.3.1	Direct formulation: the transfer matrix	4
10.3.2	Rigorous derivation of the continuation procedure	5
10.4	Exact eigenmodes and eigenvalues method	9
10.5	Numerical algorithm	11
10.5.1	R matrix for a single lamellar layer	11
10.5.2	R matrix for a stack of lamellar layers	12
10.6	Numerical application	12
10.7	Appendix. Calculation of the exact modes and eigenvalues	14
10.7.1	The equation satisfied by the exact eigenvalues	14
10.7.2	Real eigenvalues	16
10.7.3	Complex eigenvalues	17
10.7.4	Eigenfunctions	18

Exact Modal Methods

Boris Gralak

CNRS, Aix-Marseille Université, École Centrale Marseille, Institut Fresnel,
 13397 Marseille Cedex 20, France
boris.gralak@fresnel.fr

10.1 Introduction

Exact modal method (EMM) has been proposed to take advantage of geometry of lamellar gratings. These gratings are made of rectangular rods periodically spaced which can be considered locally as periodic multilayered stacks (see figure 10.1). This simple geometry makes it possible to expand the electromagnetic field on the basis of “exact modes”, and to obtain an exact representation of the permittivity. In this particular case, EMM can be more efficient than similar methods based on Fourier expansion (coupled-wave method [1] or Fourier modal method [2, 3]) which may lead to poor convergence due to the discontinuous nature of both electromagnetic field and permittivity. This advantage of EMM becomes more important when the permittivity contrast is high, e.g. for metallic lamellar gratings.

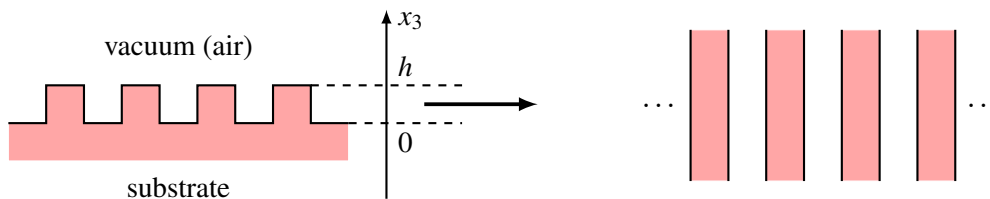


Figure 10.1: A lamellar grating made of a single lamellar layer on a substrate. The region corresponding to the lamellar layer, between the planes $x_3 = 0$ and $x_3 = h$, can be considered as the multilayered stack on the left.

Exact modal method has been introduced in 1981 in order to solve Maxwell’s equations in presence of lamellar gratings made of dielectrics [4] and metals [5, 6, 7]. Since these pioneering works, a major contribution to this method is certainly its rigorous extension to conical mountings [8], on which is based an EMM for three-dimensional woodpile structures [9]. Another major development is the introduction of perfectly matched layers in order to model aperiodic systems met in integrated optics [10] (information can be found on the website of CAMFR).

In this chapter, a rigorous formulation of the exact modal method for lamellar structures is presented. In section 10.3, a special attention is paid to the continuation of the electromagnetic

field inside a lamellar layer. In combination with the boundary conditions, this continuation provides a large class of solutions of Maxwell's equations in presence of lamellar gratings. In section 10.4, it is shown that, in each lamellar layer, there is a decoupling of the vector field equations into two independent scalar equations, which correspond to the ones of a multilayered stack (see figure 10.1). Numerical stacking algorithms are presented in section 10.5 and a numerical illustration of the EMM efficiency is proposed in section 10.6. Finally, the techniques used for the calculation of the exact modes and the associated exact eigenvalues are reported in the appendix (section 10.7).

Note that the important extensions to woodpile structures [9] and to lamellar gratings including infinitely conducting metal [11] are not considered in this book chapter. These cases will be however included in the next version.

10.2 Notations

Throughout this chapter an orthonormal basis $(\mathbf{e}_1, \mathbf{e}_2, \mathbf{e}_3)$ is used: every vector \mathbf{x} in \mathbb{R}^3 is described by its three components x_1, x_2 and x_3 . It is shown how to obtain in the presence of a stack of lamellar layers, a large class of solutions \mathbf{E} of the Helmholtz equation

$$[\omega^2 - \varepsilon^{-1} \nabla \times \mu^{-1} \nabla \times] \mathbf{E} = \mathbf{0}, \quad (10.1)$$

where ε is the permittivity, μ is the permeability, ω is the frequency and $\nabla \times$ is the curl operator. All the media considered in this chapter are isotropic, and thus the permittivity and permeability reduce to scalar functions. The considered structure is independent of the variable x_2 , and x_1 -periodic with spatial period $\mathbf{d} = d\mathbf{e}_1$:

$$\varepsilon(\mathbf{x} + \mathbf{d}) = \varepsilon(\mathbf{x}) = \varepsilon(x_1, x_3), \quad \mu(\mathbf{x} + \mathbf{d}) = \mu(\mathbf{x}) = \mu(x_1, x_3), \quad \mathbf{x} \in \mathbb{R}^3. \quad (10.2)$$

The unit cell associated with this grating is $[0, d]$ and the one-dimensional lattice is $\{n\mathbf{d} \mid n \in \mathbb{Z}\}$. Then, a *lamellar grating* is a stack in the direction x_3 of lamellar layers where ε and μ are both functions of the single variable x_1 (figure 10.2). In practice, each lamellar layer is made of infinite parallel rods with rectangular cross section (figure 10.2): the functions ε and μ are piecewise constant of the solely variable x_1 .

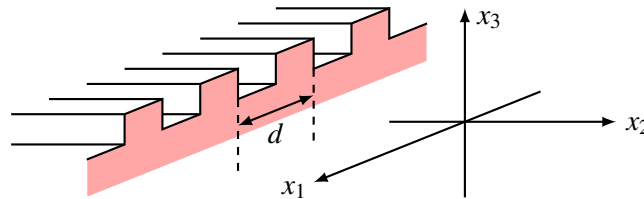


Figure 10.2: A lamellar grating made of a single lamellar layer on a substrate.

In order to obtain a set of first order differential equations from (10.1) a second field is defined:

$$\mathbf{H} = (\omega\mu)^{-1} \nabla \times \mathbf{E}. \quad (10.3)$$

Note that this quantity differs from the usual “harmonic \mathbf{H} field” by the complex number i . Solutions \mathbf{E} , \mathbf{H} are investigated in the space of fields whose restrictions in every horizontal

plane (normal to \mathbf{e}_3) are square integrable:

$$\int_{\mathbb{R}^2} |\mathbf{F}(x_1, x_2, x_3)|^2 dx_1 dx_2 < \infty, \quad x_3 \in \mathbb{R}, \quad (10.4)$$

where $\mathbf{F} = \mathbf{E}, \mathbf{H}$.

The first consequence of (10.4) is the possibility to perform a decomposition of the problem to take advantage of the spatial invariances of the system: a Fourier decomposition with respect to the variable x_2 ,

$$\mathbf{F} \longrightarrow \widehat{\mathbf{F}}(x_1, k_2, x_3) = \frac{1}{2\pi} \int_{\mathbb{R}} \exp[-ik_2 x_2] \mathbf{F}(x_1, x_2, x_3) dx_2, \quad (10.5)$$

and a Floquet-Bloch decomposition with respect to the variable x_1 ,

$$\widehat{\mathbf{F}} \longrightarrow \tilde{\mathbf{F}}(k_1, x_1, k_2, x_3) \frac{1}{2\pi} \sum_{n \in \mathbb{Z}} \exp[-ik_1 n d] \widehat{\mathbf{F}}(x_1 + pd, k_2, x_3), \quad (10.6)$$

where k_1 is the Bloch wave vector in the first Brillouin zone $[-\pi/d, \pi/d]$. Thus solutions $\tilde{\mathbf{E}}, \tilde{\mathbf{H}}$ satisfy

$$\int_{[-\pi/d, \pi/d]} |\tilde{\mathbf{F}}(k_1, x_1, k_2, x_3)|^2 dx_1 < \infty, \quad x_1, k_2, x_3 \in \mathbb{R}, \quad (10.7)$$

with the partial Bloch boundary condition

$$\tilde{\mathbf{F}}(k_1, x_1 + d, k_2, x_3) = \exp[ik_1 d] \tilde{\mathbf{F}}(k_1, x_1, k_2, x_3), \quad (10.8)$$

where k_1 is fixed in $[-\pi/d, \pi/d]$.

The second consequence of (10.4) [or (10.7)] is that the restrictions to every horizontal plane of $\nabla \times \mathbf{E}$ and $\nabla \times \mathbf{H}$ are also locally square integrable [from (10.1,10.3)]. Then, for all $i, j = 1, 2, 3$ and $i \neq j$, E_i and H_i are continuous functions of the variable x_j . In particular, the tangential components E_1, E_2, H_1 and H_2 of \mathbf{E} and \mathbf{H} are continuous functions of the variable x_3 . It follows that it is possible to solve Maxwell's equations in a stack of layers by the following two steps: the first step consists in solving Maxwell's equations in each layer independently and then the second step consists in connecting each independent solution using the continuity of E_1, E_2, H_1 and H_2 .

With the definition (10.3), equation (10.1) is equivalent to the set of first order equations

$$\mathbf{E} = (\omega\epsilon)^{-1} \nabla \times \mathbf{H}, \quad \mathbf{H} = (\omega\mu)^{-1} \nabla \times \mathbf{E}. \quad (10.9)$$

Let the 2×2 matrix σ and the two-components vector F_j defined by

$$\sigma = \omega \begin{bmatrix} 0 & \mu \\ \epsilon & 0 \end{bmatrix}, \quad F_j = \begin{bmatrix} \tilde{E}_j \\ \tilde{H}_j \end{bmatrix}, \quad j = 1, 2, 3. \quad (10.10)$$

Then, the first order equations (10.9) can be developed as

$$\begin{aligned} F_1 &= \sigma^{-1} [\partial_2 F_3 - \partial_3 F_2], \\ F_2 &= \sigma^{-1} [\partial_3 F_1 - \partial_1 F_3], \\ F_3 &= \sigma^{-1} [\partial_1 F_2 - \partial_2 F_1], \end{aligned} \quad (10.11)$$

where ∂_j is the partial derivative with respect to the variable x_j ($j = 1, 2, 3$). This last set of equations is exactly the same as (10.9) and, with some abuse of notations, it can be written in the compact way $\mathbf{F} = \sigma^{-1} \nabla \times \mathbf{F}$, with $\mathbf{F} = (F_1, F_2, F_3)$.

10.3 Continuation of the electromagnetic field

In this section two different formulations are presented to solve the equation $\mathbf{F} = \sigma^{-1} \nabla \times \mathbf{F}$ in a lamellar layer located between the planes $x_3 = 0$ and $x_3 = h$. In practice, this solution is expressed as a relationship between $\mathbf{F}(0)$ and $\mathbf{F}(h)$. Note that the formulations presented in this section remain valid in the general case of cross gratings with two-dimensional periodicity [2].

10.3.1 Direct formulation: the transfer matrix

The starting point is the set of equations (10.11). Eliminating the components F_3 , one obtains

$$\partial_3 F = iMF, \quad F = \begin{bmatrix} F_1 \\ F_2 \end{bmatrix}, \quad M = -i \begin{bmatrix} -\partial_1 \sigma^{-1} \partial_2 & \sigma + \partial_1 \sigma^{-1} \partial_1 \\ -\sigma - \partial_2 \sigma^{-1} \partial_2 & \partial_2 \sigma^{-1} \partial_1 \end{bmatrix}. \quad (10.12)$$

For a lamellar layer located between the planes $x_3 = 0$ and $x_3 = h$ (see figure 10.1), the functions ε and μ are x_3 -independent for x_3 in $[0, h]$: then the matrix σ and the operator-valued matrix M are also x_3 -independent for x_3 in $[0, h]$. Let L be the x_3 -independent operator valued matrix which coincides with M in this single layer:

$$L = M(x_3), \quad x_3 \in [0, h]. \quad (10.13)$$

In a first step, it is assumed that (see the end of section 10.4 for a justification) the matrix L has a diagonal form and can be written as

$$L = V \lambda V^{-1}, \quad (10.14)$$

where the matrix V contains the eigenvectors $V_{\pm, n}$ of L , and λ is the diagonal matrix made of the associated eigenvalues $\lambda_{\pm, n}$:

$$LV_{\pm, n} = \lambda_{\pm, n} V_{\pm, n}. \quad (10.15)$$

The sets of eigenvectors and eigenvalues are split into two parts according to the sign of the imaginary part of $\lambda_{\pm, n}$: $\text{Im} \lambda_{+, n} > 0$ and $\text{Im} \lambda_{-, n} < 0$. Let λ_+ (respectively λ_-) be the diagonal matrices containing the eigenvalues $\lambda_{+, n} > 0$ of L (respectively $\lambda_{-, n} > 0$): then

$$\lambda = \begin{bmatrix} \lambda_+ & 0 \\ 0 & \lambda_- \end{bmatrix}, \quad \text{Im} \lambda_+ > 0, \quad \text{Im} \lambda_- < 0. \quad (10.16)$$

This last condition on the imaginary part of eigenvalues is always realized if there is some absorption, *i.e.* $\text{Im} \sigma > 0$, or if a small positive imaginary part is added to the frequency ω (in the later case the limit $\omega = \lim_{\eta \downarrow 0} (\omega + i\eta)$ is considered [12, 13]). The combination of (10.12) and (10.13) leads to the equation

$$\partial_3 F(x_3) = iLF(x_3), \quad x_3 \in [0, h], \quad (10.17)$$

where the dependence on other variables has been omitted. Since L is x_3 -independent, the “formal” solution of this equation is just

$$F(x_3) = \exp[iLx_3]F(0), \quad x_3 \in [0, h]. \quad (10.18)$$

This solution is denominated by “formal” since, at this stage, it is still necessary to check if it exists. Using the diagonal form (10.14) of the operator L , the expression (10.18) becomes

$$F(x_3) = V \exp[i\lambda x_3] V^{-1} F(0). \quad (10.19)$$

Actually, the diagonal matrix $\exp[i\lambda x_3]$ is made of the two parts $\exp[i\lambda_{\pm} x_3]$ which have different behaviour. From (10.16), the part $\exp[i\lambda_+ x_3]$ is bounded by $\exp[-\text{Im}\lambda_+ x_3] < 1$. On the contrary, the part $\exp[i\lambda_- x_3]$ is not bounded and, in general, the corresponding coefficients are growing towards infinity like exponential functions. Consequently, the transfer matrix $T(x_3)$ defined by

$$F(x_3) = T(x_3)F(0), \quad T(x_3) = V \exp[i\lambda x_3] V^{-1}, \quad (10.20)$$

has “infinite” coefficients and thus expressions like (10.18), (10.19) and (10.20) have to be considered as purely “formal” and have to be handled cautiously. Numerically, the transfer matrix is truncated and, because its coefficients tend to infinity like exponential functions, it presents numerical instabilities which makes it difficult to use it. A numerical solution has been found to solve this problem with the definition of the S - and R -algorithms [14] (see section 10.5 for the numerical solution in the present case).

Finally, notice that the transfer matrix is occasionally derived from the matrix L^2 instead of L . Indeed, the assumption (10.14) on the diagonal form of L might be too strong and not rigorously true. According to notations (10.14), we denote by V and λ^2 the matrices containing the eigenvectors and eigenvalues of L^2 :

$$L^2 = V \lambda^2 V^{-1}. \quad (10.21)$$

In that case, it used that equations (10.12) and (10.13) imply

$$\partial_3^2 F = -L^2 F, \quad x_3 \in [0, h]. \quad (10.22)$$

The combination of the two last equations leads to

$$F(x_3) = V \cos[\lambda x_3] V^{-1} F(0) + V \lambda^{-1} \sin[\lambda x_3] V^{-1} (\partial_3 F)(0). \quad (10.23)$$

Replacing $(\partial_3 F)(0)$ by $iLF(0)$, one obtains for the transfer matrix the following “formal” expression

$$T(x_3) = V \cos[\lambda x_3] V^{-1} + iV \lambda^{-1} \sin[\lambda x_3] V^{-1} L. \quad (10.24)$$

This equation is not “formally” equivalent to the first expression (10.20) derived from L . This equivalence requires the assumption (10.14) to become true, so that L can be replaced by $V \lambda V^{-1}$ above (and next the formal identity $\cos[\lambda x_3] + i \sin[\lambda x_3] = \exp[i\lambda x_3]$ has to be used).

10.3.2 Rigorous derivation of the continuation procedure

A rigorous formulation is based on the use of the Fourier transform with respect to the variable x_3 defined by

$$\mathcal{F}[F](k_3) = \frac{1}{2\pi} \int_{\mathbb{R}} \exp[-ik_3 x_3] F(x_3) dx_3. \quad (10.25)$$

The function F is then deduced from its Fourier transform $\mathcal{F}[F]$ by

$$F(x_3) = \int_{\mathbb{R}} \exp[ik_3 x_3] \mathcal{F}[F](k_3) dk_3. \quad (10.26)$$

It is not suitable to perform directly the Fourier transform of the equation (10.12) since the matrix σ (and then M) is not independent of x_3 in \mathbb{R} . However, if equation (10.12) is multiplied by the characteristic function Ψ of the lamellar layer [so $\Psi(x_3) = 1$ for x_3 in $[0, h]$ and vanishes otherwise], then

$$\Psi(x_3)\partial_3 F(x_3) = \Psi(x_3)iMF(x_3) = \Psi(x_3)iLF(x_3) = iL\Psi(x_3)F(x_3). \quad (10.27)$$

After this multiplication, a partial differential equation with the x_3 -independent matrix L is obtained. The Fourier transform (10.25) of $\Psi\partial_3 F$ is

$$\begin{aligned} \mathcal{F}[\Psi\partial_3 F](k_3) &= \frac{1}{2\pi} \int_{\mathbb{R}} \exp[-ik_3 x_3] \Psi(x_3) \partial_3 F(x_3) dx_3 \\ &= \frac{1}{2\pi} \int_0^h \exp[-ik_3 x_3] \partial_3 F(x_3) dx_3 \\ &= \frac{1}{2\pi} \{ \exp[-ik_3 h] F(h) - F(0) \} + ik_3 \mathcal{F}[\Psi F](k_3), \end{aligned} \quad (10.28)$$

where the last line comes from an integration by parts. After this Fourier transform, equation (10.27) becomes

$$\frac{1}{2\pi} \{ \exp[-ik_3 h] F(h) - F(0) \} + ik_3 \mathcal{F}[\Psi F](k_3) = iL \mathcal{F}[\Psi F](k_3) \quad (10.29)$$

or

$$[k_3 - L] \mathcal{F}[\Psi F](k_3) = \frac{1}{2i\pi} \{ F(0) - \exp[-ik_3 h] F(h) \}. \quad (10.30)$$

The operator $[k_3 - L]$ is always invertible if there is some absorption, *i.e.* $\text{Im}\sigma > 0$, or if the limit $\omega = \lim_{\eta \downarrow 0} (\omega + i\eta)$ is considered (see [12, 13], this is equivalent to the property (10.16) on the eigenvalues λ since k_3 is purely real). Hence it is possible to write

$$\mathcal{F}[\Psi F](k_3) = \frac{1}{2i\pi} \frac{1}{k_3 - L} \{ F(0) - \exp[-ik_3 h] F(h) \}, \quad (10.31)$$

The final step is to apply the inverse Fourier transform (10.26): for x_3 in $[0, h]$,

$$\begin{aligned} \Psi(x_3)F(x_3) &= \frac{1}{2i\pi} \left[\int_{\mathbb{R}} \exp[ik_3 x_3] \frac{1}{k_3 - L} dk_3 \right] F(0) \\ &\quad - \frac{1}{2i\pi} \left[\int_{\mathbb{R}} \exp[ik_3 (x_3 - h)] \frac{1}{k_3 - L} dk_3 \right] F(h). \end{aligned} \quad (10.32)$$

Again, it is assumed that the operator L can be written $L = V\lambda V^{-1}$ (10.14). Replacing the matrix L by its diagonal form, the last expression becomes

$$\begin{aligned} \Psi(x_3)F(x_3) &= \frac{1}{2i\pi} V \left[\int_{\mathbb{R}} \exp[ik_3 x_3] \frac{1}{k_3 - \lambda} dk_3 \right] V^{-1} F(0) \\ &\quad - \frac{1}{2i\pi} V \left[\int_{\mathbb{R}} \exp[ik_3 (x_3 - h)] \frac{1}{k_3 - \lambda} dk_3 \right] V^{-1} F(h). \end{aligned} \quad (10.33)$$

The integrations above are performed by adding to the real axis of k_3 a semi-circle with infinite radius (in the complex plane of k_3) on which the integrals vanish. For the first term with $F(0)$,

the complex number k_3 must have positive imaginary part (x_3 is positive), so that the real axis is closed by a semi-circle in the upper half plane (see the red path on figure 10.3). In this case, the solely eigenvalues contained in λ_+ generate contributions in the integral. For the second term with $F(h)$, the complex number k_3 must have negative imaginary part ($x_3 - h$ is negative), so that the real axis is closed by a semi-circle in the lower half plane (see the blue path on figure 10.3). Here, the integral is given by the eigenvalues contained in λ_- . Let P_{\pm} be the projectors

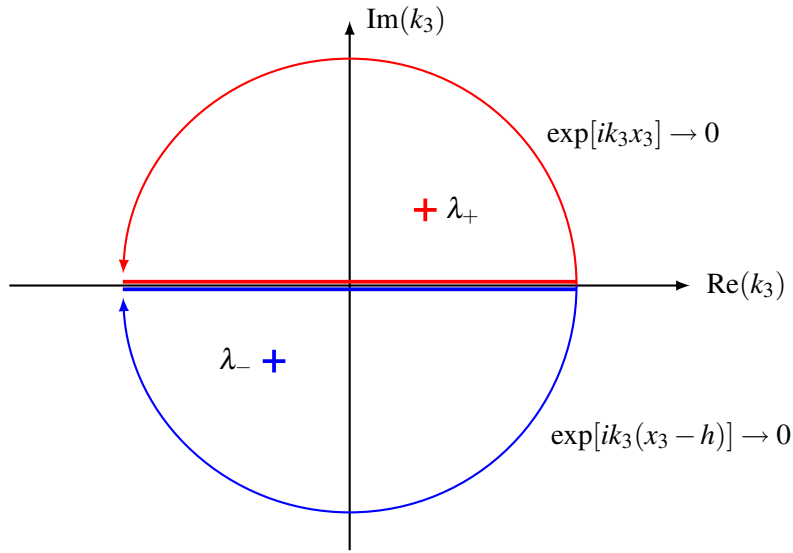


Figure 10.3: Integration in the complex plane of k_3 .

upon the spaces corresponding respectively to eigenvalues λ_{\pm} :

$$P_+ \lambda = \begin{bmatrix} \lambda_+ & 0 \\ 0 & 0 \end{bmatrix}, \quad P_- \lambda = \begin{bmatrix} 0 & 0 \\ 0 & \lambda_- \end{bmatrix}. \quad (10.34)$$

Then, after the integration over k_3 , expression (10.33) yields

$$\Psi(x_3)F(x_3) = V P_+ \exp[i\lambda_+ x_3] V^{-1} F(0) + V P_- \exp[i\lambda_- (x_3 - h)] V^{-1} F(h). \quad (10.35)$$

This expression is always well defined since the integration in the complex plane of k_3 imposes that all the complex exponential functions decrease:

$$\| \exp[i\lambda_+ x_3] \| \leq 1, \quad \| \exp[i\lambda_- (x_3 - h)] \| \leq 1. \quad (10.36)$$

Considering the rigorous expression (10.35) at $x_3 = 0$ and $x_3 = h$ and using that $P_- + P_+$ is the identity, one obtains

$$\begin{aligned} V P_- V^{-1} F(0) &= V P_- \exp[-i\lambda_- h] V^{-1} F(h), \\ V P_+ V^{-1} F(h) &= V P_+ \exp[i\lambda_+ h] V^{-1} F(0). \end{aligned} \quad (10.37)$$

These two relationships provides a rigorous way to deduce $F(0)$ from $F(h)$ and conversely.

As in the previous section, the continuation procedure is also derived from the diagonal form (10.21) of L^2 . Equation (10.22) is multiplied by $\Psi(x_3)$ to provide an expression similar to (10.27)

$$\Psi(x_3) \partial_3 F(x_3) = -L^2 \Psi(x_3) F(x_3). \quad (10.38)$$

Then, the Fourier transform (10.25) is applied to this equation. Using that

$$\begin{aligned}\mathcal{F}[\Psi\partial_3^2 F](k_3) &= \frac{1}{2\pi} \int_{\mathbb{R}} \exp[-ik_3x_3] \Psi(x_3) \partial_3^2 F(x_3) dx_3 \\ &= -k_3^2 \mathcal{F}[\Psi F](k_3) + ik_3 \frac{1}{2\pi} \{ \exp[-ik_3h]F(h) - F(0) \} \\ &\quad + \frac{1}{2\pi} \{ \exp[-ik_3h](\partial_3 F)(h) - (\partial_3 F)(0) \},\end{aligned}\tag{10.39}$$

and replacing $(\partial_3 F)(x_3)$ by $iLF(x_3)$, equation (10.38) implies

$$\begin{aligned}\mathcal{F}[\Psi F](k_3) &= \frac{1}{2i\pi} \frac{1}{k_3^2 - L^2} k_3 \{ F(0) - \exp[-ik_3h]F(h) \} \\ &= \frac{1}{2i\pi} \frac{1}{k_3^2 - L^2} \{ LF(0) - \exp[-ik_3h]LF(h) \}.\end{aligned}\tag{10.40}$$

Next, the inverse Fourier transform (10.26) is performed for x_3 in $[0, h]$ and the diagonal form (10.21) is used:

$$\begin{aligned}\Psi(x_3)F(x_3) &= \frac{1}{2i\pi} V \int_{\mathbb{R}} \frac{k_3}{k_3^2 - \lambda^2} \{ \exp[ik_3x_3]V^{-1}F(0) - \exp[ik_3(x_3 - h)]V^{-1}F(h) \} dx_3 \\ &\quad + \frac{1}{2i\pi} V \int_{\mathbb{R}} \frac{1}{k_3^2 - \lambda^2} \{ \exp[ik_3x_3]V^{-1}LF(0) - \exp[ik_3(x_3 - h)]V^{-1}LF(h) \} dx_3.\end{aligned}\tag{10.41}$$

Again, the integrations above are calculated by adding to the real axis of k_3 a semi-circle with infinite radius (in the complex plane of k_3) on which the integrals vanish. Without loss of generality, it is considered that the square root of the eigenvalues in λ^2 have non-zero imaginary part: let $\sqrt{\lambda^2}$ be the square root of λ^2 with positive imaginary part. For the terms with $F(0)$, the real axis is closed by a semi-circle in the upper half plane, and the eigenvalues with positive imaginary part $\sqrt{\lambda^2}$ lead to contributions in the integrals. For the terms with $F(h)$, the real axis is closed by a semi-circle in the lower half plane, and the integrals are given by the eigenvalues with negative imaginary part, *i.e.* $-\sqrt{\lambda^2}$. Calculations of integrals over k_3 lead to

$$\begin{aligned}\Psi(x_3)F(x_3) &= V \frac{1}{2} \exp[i\sqrt{\lambda^2}x_3]V^{-1}F(0) + V \frac{1}{2} \exp[-i\sqrt{\lambda^2}(x_3 - h)]V^{-1}F(h) \\ &\quad + V \frac{1}{2\sqrt{\lambda^2}} \exp[i\sqrt{\lambda^2}x_3]V^{-1}LF(0) - V \frac{1}{2\sqrt{\lambda^2}} \exp[-i\sqrt{\lambda^2}(x_3 - h)]V^{-1}LF(h).\end{aligned}\tag{10.42}$$

This equation is evaluated at $x_3 = 0$ and $x_3 = h$:

$$\begin{aligned}F(0) &= V \exp[i\sqrt{\lambda^2}h]V^{-1}F(h) + V \frac{1}{\sqrt{\lambda^2}} V^{-1}LF(0) - V \frac{1}{\sqrt{\lambda^2}} \exp[i\sqrt{\lambda^2}h]V^{-1}LF(h), \\ F(h) &= V \exp[i\sqrt{\lambda^2}h]V^{-1}F(0) + V \frac{1}{\sqrt{\lambda^2}} \exp[i\sqrt{\lambda^2}h]V^{-1}LF(0) - V \frac{1}{\sqrt{\lambda^2}} V^{-1}LF(h).\end{aligned}\tag{10.43}$$

Thanks to the technique based on the Fourier transform, all the exponential functions in these expressions must be well-defined. Indeed, the imaginary part of $\sqrt{\lambda^2}$ is positive and all the exponential functions decrease. Equations (10.43) will be used to construct a stable numerical algorithm to stack several lamellar layers.

10.4 Exact eigenmodes and eigenvalues method

The different solutions (10.20), (10.24), (10.37) and (10.43), established in the previous section, are provided from the knowledge of the sets of eigenmodes and eigenvalues of the operator L (or L^2). In this section, it is shown how these eigenmodes $V_{\pm,n}$ and eigenvalues $\lambda_{\pm,n}$ of L can be exactly determined in a lamellar layer located between the planes $x = 0$ and $x_3 = h$. The starting point is equation (10.17):

$$\partial_3 F = iLF, \quad L = M(x_3), \quad x_3 \in [0, h]. \quad (10.44)$$

Let ε_1 , μ_1 and σ_1 be the functions which coincide with respectively ε , μ and σ in the considered lamellar layer for x_3 in $[0, h]$. In the considered lamellar layer, they are functions of the solely variable x_1 (see figure 10.2):

$$\varepsilon_1(x_1) = \varepsilon(x_1, x_3), \quad \mu_1(x_1) = \mu(x_1, x_3), \quad \sigma_1(x_1) = \sigma(x_1, x_3), \quad x_3 \in [0, h]. \quad (10.45)$$

According to expression (10.12), the operator L is now

$$L = -i \begin{bmatrix} -\partial_1 \sigma_1^{-1} \partial_2 & \sigma_1 + \partial_1 \sigma_1^{-1} \partial_1 \\ -\sigma_1 - \partial_2 \sigma_1^{-1} \partial_2 & \partial_2 \sigma_1^{-1} \partial_1 \end{bmatrix}, \quad (10.46)$$

and its square is

$$L^2 = - \begin{bmatrix} -\sigma_1^2 - \partial_1 \sigma_1^{-1} \partial_1 \sigma_1 - \sigma_1 \partial_2 \sigma_1^{-1} \partial_2 & \sigma_1 \partial_2 \sigma_1^{-1} \partial_1 - \partial_1 \sigma_1^{-1} \partial_2 \sigma_1 \\ \sigma_1 \partial_1 \sigma_1^{-1} \partial_2 - \partial_2 \sigma_1^{-1} \partial_1 \sigma_1 & -\sigma_1^2 - \partial_2 \sigma_1^{-1} \partial_2 \sigma_1 - \sigma_1 \partial_1 \sigma_1^{-1} \partial_1 \end{bmatrix}. \quad (10.47)$$

Since the matrix σ_1 is x_2 -independent, the equality $\sigma_1 \partial_2 \sigma_1^{-1} = \partial_2 = \sigma_1^{-1} \partial_2 \sigma_1$ holds, and the expression above becomes

$$L^2 = \begin{bmatrix} \sigma_1^2 + \partial_2^2 + \partial_1 \sigma_1^{-1} \partial_1 \sigma_1 & 0 \\ \partial_2 \sigma_1^{-1} \partial_1 \sigma_1 - \sigma_1 \partial_1 \sigma_1^{-1} \partial_2 & \sigma_1^2 + \partial_2^2 + \sigma_1 \partial_1 \sigma_1^{-1} \partial_1 \end{bmatrix}. \quad (10.48)$$

This expression shows that the components F_1 can be decoupled from the components F_2 in the lamellar layer. Indeed, it implies

$$\partial_3^2 F_1 = -KF_1, \quad K = \sigma_1^2 + \partial_2^2 + \partial_1 \sigma_1^{-1} \partial_1 \sigma_1. \quad (10.49)$$

Moreover, each component of F_1 , *i.e.* E_1 and H_1 , can be also decoupled since the operator K is diagonal:

$$K = \begin{bmatrix} K_{\varepsilon_1} & 0 \\ 0 & K_{\mu_1} \end{bmatrix}, \quad (10.50)$$

where

$$\begin{aligned} K_{\varepsilon_1} &= \omega^2 \varepsilon_1 \mu_1 + \partial_2^2 + \partial_1 \varepsilon_1^{-1} \partial_1 \varepsilon_1, \\ K_{\mu_1} &= \omega^2 \varepsilon_1 \mu_1 + \partial_2^2 + \partial_1 \mu_1^{-1} \partial_1 \mu_1. \end{aligned} \quad (10.51)$$

Here, it is important to notice that the two operators K_{ε_1} and K_{μ_1} correspond to the ones of a one-dimensional multilayered stack for respectively p - and s -polarization. This makes it possible to calculate the exact eigenmodes and eigenvalues of K_{ε_1} and K_{μ_1} (see appendix) and thus the ones of K . Thus the continuation procedure presented in section 10.3.2 can be applied to

equation (10.49). It provides relationships between the fields $F_1(0)$, $F_1(h)$ and their derivative with respect to x_3 , *i.e.* $[\partial_3 F_1](0)$ and $[\partial_3 F_1](h)$ (it is recalled that $\partial_3 F = iLF$ in section 10.3.2).

To complete the derivation of the method, it is necessary to express the component F_2 of the field from F_1 and $\partial_3 F_1$. A starting relationship is obtained from (10.44) and (10.47):

$$\partial_3 F_1 = -\partial_1 \sigma_1^{-1} \partial_2 F_1 + [\sigma_1 + \partial_1 \sigma_1^{-1} \partial_1] F_2. \quad (10.52)$$

This equation is equivalent to

$$[1 + \partial_1 \sigma_1^{-1} \partial_1 \sigma_1^{-1}] \sigma_1 F_2 = \partial_3 F_1 + \partial_1 \sigma_1^{-1} \partial_2 F_1. \quad (10.53)$$

Here, it is remarked that the operator $[1 + \partial_1 \sigma_1^{-1} \partial_1 \sigma_1^{-1}]$ is invertible since it equals $[K - \partial_2^2] \sigma_1^{-2}$ where σ_1 is invertible as well as $[K - \partial_2^2]$ (eigenvalues of K have non-zero imaginary part). Moreover, the operator $[1 + \partial_1 \sigma_1^{-1} \partial_1 \sigma_1^{-1}]$ commutes with ∂_3 , ∂_2 and $\partial_1 \sigma_1^{-1}$: hence

$$\begin{aligned} \sigma_1 F_2 &= \frac{1}{1 + \partial_1 \sigma_1^{-1} \partial_1 \sigma_1^{-1}} \partial_3 F_1 + \frac{1}{1 + \partial_1 \sigma_1^{-1} \partial_1 \sigma_1^{-1}} \partial_1 \sigma_1^{-1} \partial_2 F_1 \\ &= \frac{1}{1 + \partial_1 \sigma_1^{-1} \partial_1 \sigma_1^{-1}} \partial_3 F_1 + \partial_2 \partial_1 \sigma_1^{-1} \frac{1}{1 + \partial_1 \sigma_1^{-1} \partial_1 \sigma_1^{-1}} F_1 \\ &= \sigma_1^2 \frac{1}{\sigma_1^2 + \partial_1 \sigma_1^{-1} \partial_1 \sigma_1} \partial_3 F_1 + \partial_2 \partial_1 \sigma_1 \frac{1}{\sigma_1^2 + \partial_1 \sigma_1^{-1} \partial_1 \sigma_1} F_1. \end{aligned} \quad (10.54)$$

After the Fourier decomposition with respect to the variable x_2 , the operator ∂_2 becomes ik_2 . Then, the inverse operator above is expressed using the diagonal form $K = V\lambda^2 V^{-1}$, and the component F_2 becomes

$$F_2 = \sigma_1 V \frac{1}{\lambda^2 + k_2^2} V^{-1} \partial_3 F_1 + ik_2 \sigma_1^{-1} \partial_1 \sigma_1 V \frac{1}{\lambda^2 + k_2^2} V^{-1} F_1. \quad (10.55)$$

Finally, it is stressed that the coefficients of the operators $\sigma_1 V$ and $\sigma_1^{-1} \partial_1 \sigma_1 V$ above can be calculated exactly from the knowledge of the exact eigenmodes. Indeed, the technique presented in appendix shows that the determination of the eigenmodes ϕ_n lies on the calculations of functions $\sigma_1 \phi_n$ and $\sigma_1^{-1} \partial_1 \sigma_1 \phi_n$. The final expression of F_2 in terms of F_1 and $\partial_3 F_1$ is then

$$F_2 = U \frac{1}{\lambda^2 + k_2^2} V^{-1} \partial_3 F_1 + ik_2 W \frac{1}{\lambda^2 + k_2^2} V^{-1} F_1, \quad U = \sigma_1 V, \quad W = \sigma_1^{-1} \partial_1 \sigma_1 V. \quad (10.56)$$

To conclude this section, it has been shown that the field components F_1 , $\partial_3 F_1$ and F_2 can be expressed exactly in a lamellar layer: F_1 and $\partial_3 F_1$ are provided by equations (10.42) and (10.43) (where $F \rightarrow F_1$, $LF \rightarrow -i\partial_3 F_1$, and $K = V\lambda^2 V^{-1}$); F_2 is given by equation (10.56). These expressions are based on the knowledge of the eigenvectors V of K , the eigenvalues λ^2 of K and the operators $U = \sigma_1 V$ and $W = \sigma_1^{-1} \partial_1 \sigma_1 V$. All these quantities can be calculated exactly, as shown in appendix.

Finally, it is stressed that the propagation constants inside the lamellar layer are the square roots of the eigenvalues of the operator K , *i.e.* $\pm\sqrt{\lambda^2}$. If there is some absorption, *i.e.* $\text{Im}\sigma > 0$, or if a small positive imaginary part is added to the frequency ω (the limit $\omega = \lim_{\eta \downarrow 0} (\omega + i\eta)$ is considered [12, 13]), the eigenvalues λ^2 of K cannot be purely real. It follows that the propagation constants $\pm\sqrt{\lambda^2}$ have non zero imaginary parts and, moreover, the half of them ($+\sqrt{\lambda^2}$) have strictly positive imaginary part and the second half of them ($-\sqrt{\lambda^2}$) have strictly negative imaginary part. In this case, the assumption (10.16) on the eigenvalues of L is well justified.

10.5 Numerical algorithm

A general solution for numerical algorithm has been proposed by L. Li in the case of modal methods of gratings [3]. This solution is based on the definition of S or R matrices which are well-conditioned.

10.5.1 R matrix for a single lamellar layer

In this section, the expression of a R matrix associated with a lamellar layer is established: it is defined by the relationship

$$\begin{bmatrix} F_1(0) \\ F_1(h) \end{bmatrix} = R \begin{bmatrix} F_2(0) \\ F_2(h) \end{bmatrix}. \quad (10.57)$$

First, equation (10.43) is used to provide an expression of the solution of (10.49):

$$\begin{aligned} F_1(0) - V \exp[i\sqrt{\lambda^2}h]V^{-1}F_1(h) &= -iV \frac{1}{\sqrt{\lambda^2}} V^{-1} \partial_3 F_1(0) + iV \frac{1}{\sqrt{\lambda^2}} \exp[i\sqrt{\lambda^2}h]V^{-1} \partial_3 F_1(h), \\ F_1(h) - V \exp[i\sqrt{\lambda^2}h]V^{-1}F_1(0) &= -iV \frac{1}{\sqrt{\lambda^2}} \exp[i\sqrt{\lambda^2}h]V^{-1} \partial_3 F_1(0) + iV \frac{1}{\sqrt{\lambda^2}} V^{-1} \partial_3 F_1(h). \end{aligned} \quad (10.58)$$

This set of equations is written using 2×2 matrices:

$$A \begin{bmatrix} F_1(0) \\ F_1(h) \end{bmatrix} = B \begin{bmatrix} \partial_3 F_1(0) \\ \partial_3 F_1(h) \end{bmatrix}, \quad (10.59)$$

where

$$A = \begin{bmatrix} 1 & -V \exp[i\sqrt{\lambda^2}h]V^{-1} \\ -V \exp[i\sqrt{\lambda^2}h]V^{-1} & 1 \end{bmatrix} \quad (10.60)$$

and

$$B = \begin{bmatrix} -iV \frac{1}{\sqrt{\lambda^2}} V^{-1} & iV \frac{1}{\sqrt{\lambda^2}} \exp[i\sqrt{\lambda^2}h]V^{-1} \\ -iV \frac{1}{\sqrt{\lambda^2}} \exp[i\sqrt{\lambda^2}h]V^{-1} & iV \frac{1}{\sqrt{\lambda^2}} V^{-1} \end{bmatrix}. \quad (10.61)$$

Next, from (10.56), the field $\partial_3 F_1$ is related to F_1 and F_2 from

$$\partial_3 F_1 = -ik_2 V [\lambda^2 + k_2^2] U^{-1} W \frac{1}{\lambda^2 + k_2^2} V^{-1} F_1 + V [\lambda^2 + k_2^2] U^{-1} F_2. \quad (10.62)$$

Defining the two matrices

$$C = \begin{bmatrix} -ik_2 V [\lambda^2 + k_2^2] U^{-1} W \frac{1}{\lambda^2 + k_2^2} V^{-1} & 0 \\ 0 & -ik_2 V [\lambda^2 + k_2^2] U^{-1} W \frac{1}{\lambda^2 + k_2^2} V^{-1} \end{bmatrix} \quad (10.63)$$

and

$$D = \begin{bmatrix} V [\lambda^2 + k_2^2] U^{-1} & 0 \\ 0 & V [\lambda^2 + k_2^2] U^{-1} \end{bmatrix}, \quad (10.64)$$

the relationship (10.59) becomes

$$A \begin{bmatrix} F_1(0) \\ F_1(h) \end{bmatrix} = BC \begin{bmatrix} F_1(0) \\ F_1(h) \end{bmatrix} + BD \begin{bmatrix} F_2(0) \\ F_2(h) \end{bmatrix}. \quad (10.65)$$

Finally, according to the definition (10.57), the R matrix is given by

$$R = \frac{1}{A - BC} BD. \quad (10.66)$$

It is stressed that the R matrix is numerically stable. Indeed, exponential functions always have arguments such that they decrease and, when inverted, they are always added to well-conditioned functions. For example, in the matrix $[A - BC]$, one can check that the diagonal blocs are well-conditioned since they do not contain any exponential function, while the off-diagonal blocs decrease exponentially. When inverted, this matrix will have the same behaviour with well-conditioned diagonal blocs and exponentially decreasing off-diagonal blocs.

10.5.2 R matrix for a stack of lamellar layers

Here, a system made of two lamellar layers is considered. The first layer is located between the planes $x_3 = -h_1$ and $x_3 = 0$, and the second layer between the planes $x_3 = 0$ and $x_3 = h_2$. Let R_1 and R_2 be the R matrices associated with these layers:

$$\begin{bmatrix} F_1(-h_1) \\ F_1(0) \end{bmatrix} = R_1 \begin{bmatrix} F_2(-h_1) \\ F_2(0) \end{bmatrix}, \quad \begin{bmatrix} F_1(0) \\ F_1(h_2) \end{bmatrix} = R_2 \begin{bmatrix} F_2(0) \\ F_2(h_2) \end{bmatrix}. \quad (10.67)$$

Then, the R matrix associated with the stack of the two layers is determined by eliminating the components $F_1(0)$ and $F_2(0)$ in the equations above. Denoting by $R_{1,ij}$ and $R_{2,ij}$ ($i, j = 1, 2$) the blocs of R_1 and R_2 ,

$$R_1 = \begin{bmatrix} R_{1,11} & R_{1,12} \\ R_{1,21} & R_{1,22} \end{bmatrix}, \quad R_2 = \begin{bmatrix} R_{2,11} & R_{2,12} \\ R_{2,21} & R_{2,22} \end{bmatrix}, \quad (10.68)$$

the expression of R is given by

$$R = \begin{bmatrix} R_{1,11} - R_{1,12} \frac{1}{R_{1,22} - R_{2,11}} R_{1,21} & R_{1,12} \frac{1}{R_{1,22} - R_{2,11}} R_{2,12} \\ -R_{2,21} \frac{1}{R_{1,22} - R_{2,11}} R_{1,21} & R_{2,22} - R_{2,21} \frac{1}{R_{1,22} - R_{2,11}} R_{2,12} \end{bmatrix}. \quad (10.69)$$

Again, one can check that the algorithm is stable since the only inverted blocs are the diagonal ones, which are well-conditioned.

10.6 Numerical application

A simple numerical example is considered to put the exact modal method to the test. The structure is made of a set of rectangular rods with dielectric constant $\epsilon_{1,1}/\epsilon_0 = 12.96$ (corresponding to the index 3.6 of Si at optical wavelengths), width $w_{1,1} = 0.28d$ and height $h = d/(2\sqrt{2})$, where d is the spatial period of the grating (see figure 10.4). This lamellar grating

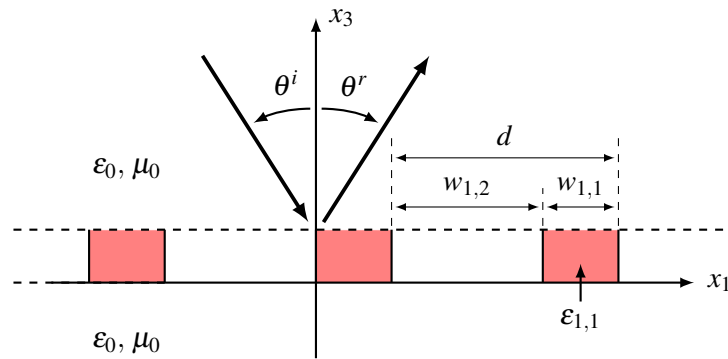


Figure 10.4: The considered structure for the numerical example: a single layer made of rectangular rods.

is illuminated by a plane wave with an incident angle $\theta^i = 45^\circ$. The oscillating frequency is $\omega = 2\pi/(d\sqrt{\epsilon_0\mu_0})$, which corresponds to a wavelength equal to the spatial period d . The efficiency diffracted in the order zero, *i.e.* at the reflected angle $\theta^r = \theta^i = 45^\circ$ is calculated for both *s* and *p*-polarizations which correspond respectively to the electric and magnetic fields reduced to a single component along the invariance axis x_2 . Each component of the electromagnetic field is described by a finite number $(2n + 1)$ of exact modes. Reflected efficiency in the order zero

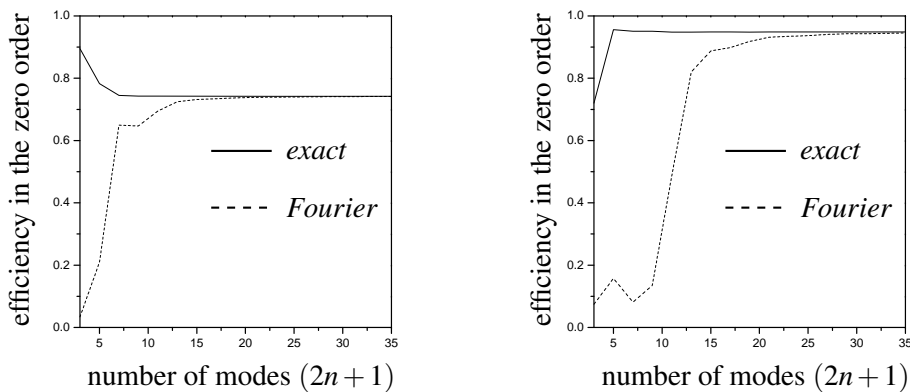


Figure 10.5: Efficiency in the zero order for *s*-polarization (left panel) and *p*-polarization (right panel).

for different values of the number of exact modes $(2n + 1)$ is represented on figure 10.5. These curves show that these efficiencies differ from their converged value with less than one percent from $(2n + 1) = 7$ in *s*-polarization and $(2n + 1) = 5$ in *p*-polarization (the converged values are respectively 0.7323 and 0.9487 in *s* and *p* polarizations). This convergence is found to be faster than in the case of the modal method with Fourier basis [2] where an error smaller than one percent is obtained from $(2n + 1) = 17$ and $(2n + 1) = 27$ in *s* and *p* polarizations respectively (the method [2] contains all the techniques to improve the convergence of the truncated Fourier series [15]). This improvement of the convergence resulting from the use of the exact modes

becomes a significant advantage when three dimensional woodpile structures are considered [9] (the total number of modes $(2n + 1)^2$ can be reduced by a factor of 10).

10.7 Appendix. Calculation of the exact modes and eigenvalues

It is shown here how to determine exactly the eigenvalues and the eigenfunctions of the operator K associated with a lamellar layer in a very general case. An analogous reasoning provides the ones of the operator associated with the others lamellar layers.

From the expression (10.50), every eigenvalue Λ_n of the operator K is either an eigenvalue of K_{ε_1} or K_{μ_1} . So, it is sufficient to determine the set of eigenvalues $\{\Lambda_{v_1, n} | n \in \mathbb{N}\}$ associated with the set of eigenfunctions $\{\phi_{v_1, n} | n \in \mathbb{N}\}$ of the scalar operator K_{v_1} , with $v_1 = \varepsilon_1$ or $v_1 = \mu_1$.

10.7.1 The equation satisfied by the exact eigenvalues

From the expression (10.50), the operator K_{v_1} is the sum of $\omega^2 \varepsilon_1 \mu_1 + \partial_1 v_1^{-1} \partial_1 v_1$ and ∂_2^2 : the first part is an operator of the single variable x_1 and the second part is an operator of the single variable x_2 . Thus, we can perform a variable separation: every eigenfunction of L_{v_1} can be written

$$\phi_{v_1, n}(x_1, x_2) = \phi_{n_1}^{(1)}(x_1) \phi_{n_2}^{(2)}(x_2) \quad n_1, n_2 \in \mathbb{N}, \quad (10.70)$$

where $\phi_{n_1}^{(1)}$ and $\phi_{n_2}^{(2)}$ are respectively eigenfunctions of the first and second operators which constitute L_{v_1} .

In the case of a lamellar grating which is invariant in the direction x_2 , this direction of invariance is considered using the Fourier decomposition (10.5). Thus the eigenfunction of ∂_2^2 is just

$$\phi_{n_2}^{(2)}(x_2) = \exp[ik_2 x_2] \quad k_2 \in \mathbb{R}, \quad (10.71)$$

and the integer n_2 plays no role (integer n will be simply n_1). In the case of woodpile crystals, it is easy to verify that the plane-wave

$$\phi_{n_2}^{(2)}(x_2) = \exp\{i[k_2 + 2\pi p(n_2)/d_2]x_2/d_2\} \quad p(n_2) \in \mathbb{Z} \quad (10.72)$$

is an eigenfunction of the operator ∂_2^2 and satisfies the partial Bloch boundary condition (10.8) adapted for the variable x_2 . Let $\Lambda_{n_2}^{(2)}$ be the associated eigenvalue. Then, from (10.71, 10.72),

$$\Lambda_{n_2}^{(2)} = -[k_2 + 2\pi q(n_2)/d_2]^2. \quad (10.73)$$

Note that, for lamellar gratings and eigenfunctions (10.71), the integer $q(n_2)$ is set to zero.

The x_1 -dependency of the eigenfunction (10.70) is determined using the usual transfer matrix [16, 17, 18]. Let $\lambda_{n_1}^{(1)}$ be the eigenvalue associated with $\phi_{n_1}^{(1)}$:

$$[\omega^2 \varepsilon_1 \mu_1 + \partial_1 v_1^{-1} \partial_1 v_1] \phi_{n_1}^{(1)} = \Lambda_{n_1}^{(1)} \phi_{n_1}^{(1)}. \quad (10.74)$$

In order to obtain a set of first order differential equations, the following column vector is introduced

$$F_{n_1} = \begin{bmatrix} v_1 \phi_{n_1}^{(1)} \\ v_1^{-1} \partial_1 v_1 \phi_{n_1}^{(1)} \end{bmatrix}. \quad (10.75)$$

Note that, from equation (10.74), the two components of this vector are continuous functions. Now, suppose that the unit cell of the considered lamellar layer is made of J rods of width $w_{1,j}$, permittivity $\varepsilon_{1,j}$ and permeability $\mu_{1,j}$, $j = 1, 2, \dots, J$ (figure 10.6): we denote by $v_{1,j}$ the value

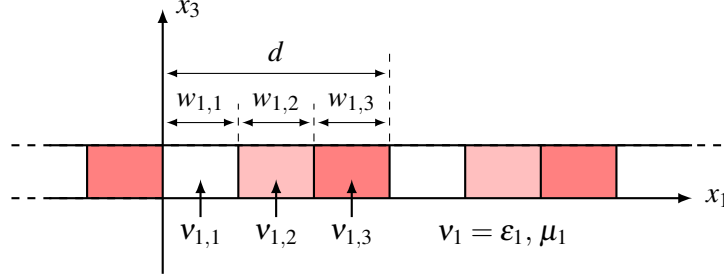


Figure 10.6: A layer made of three rods per unit cell ($J = 3$): the three rods have width $w_{1,j}$, permittivity $\varepsilon_{1,j}$ and permeability $\mu_{1,j}$, $j = 1, 2, 3$.

of the function v_1 in the rod j , $j = 1, 2, \dots, J$. Then, from equation (10.74), the vector (10.75) satisfies [18]

$$F_{n_1}(d) = T_1(\Lambda_{n_1}^{(1)})F_{n_1}(0), \quad (10.76)$$

where

$$T_1(\Lambda) = T_{1,J}(\Lambda) T_{1,J-1}(\Lambda) \cdots T_{1,1}(\Lambda), \quad (10.77)$$

$$T_{1,j}(\Lambda) = P_{1,j}(\Lambda, w_{1,j}), \quad (10.78)$$

$$P_{1,j}(\Lambda, w) = \begin{bmatrix} \cos(\beta_{1,j}w) & v_{1,j}\beta_{1,j}^{-1}\sin(\beta_{1,j}w) \\ -v_{1,j}^{-1}\beta_{1,j}\sin(\beta_{1,j}w) & \cos(\beta_{1,j}w) \end{bmatrix}, \quad (10.79)$$

$$\beta_{1,j} = \sqrt{\omega^2 \varepsilon_{1,j} \mu_{1,j} - \Lambda} \quad j = 1, 2, \dots, J. \quad (10.80)$$

Note that the four elements of each matrix $T_{1,j}$ only depend on $\beta_{1,j}^2$: the expression (10.79) is independent of the definition of the square root (10.80). In addition to (10.76), the vector (10.75) has to satisfy the partial Bloch boundary condition (10.8) for the variable x_1 :

$$F_{n_1}(d) = \exp[ik_1 d]F_{n_1}(0). \quad (10.81)$$

The combination of (10.76) and (10.81) implies that $\exp[ik_1 d]$ is an eigenvalue of the matrix $T_1(\Lambda_{n_1}^{(1)})$: the equation

$$\det \{ T_1(\Lambda_{n_1}^{(1)}) - \exp[ik_1 d] \} = 0 \quad (10.82)$$

determines the eigenvalues $\Lambda_{n_1}^{(1)}$. This last equation can be simplified using the fact that $\det T_1 = 1$ (since, from (10.78), $\det T_{1,j} = 1$, $j = 1, 2, \dots, J$): if $\exp[ik_1 d]$ is an eigenvalue of T_1 , then $\exp[-ik_1 d]$ is also. Thus, the equation (10.82) is equivalent to

$$\text{tr} T_1(\Lambda_{n_1}^{(1)}) - 2 \cos[k_1 d] = 0, \quad (10.83)$$

where $\text{tr}T_1$ is the trace of matrix T_1 . Once the eigenvalues $\Lambda_{n_1}^{(1)}$ are determined from (10.83), the associated eigenvectors $\phi_{n_1}^{(1)}$ are also obtained using the transfer matrix [17]: firstly, the eigenvector $F_{n_1}(0)$ in \mathbb{C}^2 (associated with the eigenvalue $\exp[ik_1d]$) of the matrix $T_1(\Lambda_{n_1}^{(1)})$ is determined; secondly, the expression of $\phi_{n_1}^{(1)}$ in the rod j can be deduced from

$$F_{n_1}(x_1) = P_{1,j}(\Lambda_{n_1}^{(1)}, x_1 - x_{1,j})F_{n_1}(x_{1,j-1}), \quad (10.84)$$

where

$$x_{1,0} = 0, \quad x_{1,j} = \sum_{q=1}^j w_{1,q} \quad j = 1, 2, \dots, J. \quad (10.85)$$

Finally the eigenvalues of the operator K_{v_1} are

$$\lambda_{v_1,n} = \lambda_{n_1}^{(1)} + \lambda_{n_2}^{(2)}, \quad (10.86)$$

whose the two parts are respectively given by (10.83) and (10.73), and the expression of associated eigenvectors is (10.70) whose the two parts are respectively given by (10.84) and (10.72). Concerning the functions of the operators $U = \sigma_1 V$ and $W = \sigma_1^{-1} \partial_1 \sigma_1 V$ used in section 10.4 [see equation (10.56)], they are equal to the functions

$$(v_1 \phi_{n_1}^{(1)})(x_1) \phi_{n_2}^{(2)}(x_2), \quad (v_1^{-1} \partial_1 v_1 \phi_{n_1}^{(1)})(x_1) \phi_{n_2}^{(2)}(x_2), \quad (10.87)$$

where n_1 and n_2 are in \mathbb{N} , the expression of $v_1 \phi_{n_1}^{(1)}$ and $v_1^{-1} \partial_1 v_1 \phi_{n_1}^{(1)}$ in the rod j can be deduced from (10.75,10.84) and the expression of $\phi_{n_2}^{(2)}$ is given by (10.72).

10.7.2 Real eigenvalues

Here, we suppose that the permittivity and permeability are real positive functions:

$$\varepsilon_1(x_1) \in \mathbb{R}, \quad \varepsilon_+ > \varepsilon_1(x_1) > 0; \quad \mu_1(x_1) \in \mathbb{R}, \quad \mu_+ > \mu_1(x_1) > 0. \quad (10.88)$$

Under these conditions, the operator K_{v_1} is selfadjoint and its eigenvalues are real when the following inner product is used:

$$(\phi, \psi) \longrightarrow \frac{1}{d} \int_0^d v_1(x_1) \overline{\phi(x_1)} \psi(x_1) dx_1. \quad (10.89)$$

The only difficulty in the numerical determination of the eigenvalues (10.86) is to find the real numbers $\lambda_{n_1}^{(1)}$ which satisfy the transcendental equation (10.83).

Since the numbers $\Lambda_{n_1}^{(1)}$ are eigenvalues of the operator $\omega^2 \varepsilon_1 \mu_1 + \partial_1 v_1^{-1} \partial_1 v_1 \leq \omega^2 \varepsilon_+ \mu_+$, these numbers are on the semi-axis $(-\infty, \omega^2 \varepsilon_+ \mu_+]$. This property makes their numerical determination easier and provides a way to number them:

$$\omega^2 \varepsilon_+ \mu_+ \geq \Lambda_{v_1,1} \geq \Lambda_{v_1,2} \cdots \geq \Lambda_{v_1,n} \geq \cdots \quad (10.90)$$

However, two difficulties can occur in this numerical determination. We give herein the solutions we have adopted.

The first difficulty comes from the possibility for two consecutive numbers $\Lambda_{n_1}^{(1)}$ to be very close to each other. Our solution is to use an algorithm which determines the zeros of the function $\text{tr}T_1(\Lambda) - 2\cos[k_1d]$ on the left side of equation (10.83) by taking into account this function together with its derivative with respect to Λ . If two numbers $\Lambda_{n_1}^{(1)}$ are very close one to each other, then the derivative is close to zero. Thus such algorithm needs to determine the function

$$\frac{d}{d\Lambda} \{ \text{tr}T_1(\Lambda) - 2\cos[k_1d] \} = \text{tr} \frac{dT_1}{d\Lambda}(\lambda). \quad (10.91)$$

The expression of the derivative of the matrix T_1 can be deduced from (10.77,10.78):

$$\frac{dT_1}{d\Lambda} = \frac{dT_{1,J}}{d\Lambda} T_{1,J-1} \cdots T_{1,1} + T_{1,J} \frac{dT_{1,J-1}}{d\Lambda} \cdots T_{1,1} + \cdots + T_{1,J} T_{1,J-1} \cdots \frac{dT_{1,1}}{d\Lambda}, \quad (10.92)$$

where, for $j = 1, 2, \dots, J$, the derivative of matrices

$$\frac{dT_{1,j}}{d\Lambda} = \frac{1}{2} \begin{bmatrix} a_{1,j} & b_{1,j} \\ c_{1,j} & d_{1,j} \end{bmatrix} \quad (10.93)$$

is given by

$$\begin{aligned} a_{1,j} &= w_{1,j} \beta_{1,j}^{-1} \sin[\beta_{1,j} w_{1,j}], \\ b_{1,j} &= v_{1,j} \beta_{1,j}^{-3} \sin[\beta_{1,j} w_{1,j}] - v_{1,j} w_{1,j} \beta_{1,j}^{-2} \cos[\beta_{1,j} w_{1,j}], \\ c_{1,j} &= v_{1,j}^{-1} \beta_{1,j}^{-1} \sin[\beta_{1,j} w_{1,j}] + v_{1,j}^{-1} w_{1,j} \cos[\beta_{1,j} w_{1,j}], \\ d_{1,j} &= w_{1,j} \beta_{1,j}^{-1} \sin[\beta_{1,j} w_{1,j}]. \end{aligned} \quad (10.94)$$

The second difficulty comes from the possibility of numerical instabilities in the expressions (10.79,10.93) since the numbers $\beta_{1,j}$ (10.80) can have non-vanishing imaginary part. A solution is to multiply the four coefficients of matrices $T_{1,j}$ and their derivative (10.93) by the number

$$N_j = \exp[-|\text{Im}(\beta_{1,j})| w_{1,j}] \quad j = 1, 2, \dots, J, \quad (10.95)$$

and the term $2\cos[k_1d]$ which appears in (10.83) by the product

$$N = N_J N_{J-1} \cdots N_1. \quad (10.96)$$

10.7.3 Complex eigenvalues

Here, the permittivity and permeability can take any complex value: $v_{1,j}$ is in \mathbb{C} , where $v_1 = \epsilon_1, \mu_1$ and $j = 1, 2, \dots, J$. The operator K_{v_1} is not selfadjoint and then, its eigenvalues are, in general, in the complex plane. The determination of these complex eigenvalues $\lambda_{n_1}^{(1)}$ which satisfy the equation (10.83) has been intensively studied using different methods [6, 7, 19].

We present here a method similar to the one presented in [7]: the complex eigenvalues are deduced from the real eigenvalues by an analytic continuation. However, our method differs from the one presented in [7] since we make varying the phase of the numbers $v_{1,j}$ instead of their imaginary part. We think that it is better to make varying the phase since, from that we have observed, it leaves invariant the generalization to the complex case

$$\text{Re}(\Lambda_{v_1,1}) \geq \text{Re}(\Lambda_{v_1,2}) \cdots \geq \text{Re}(\Lambda_{v_1,p}) \cdots \quad (10.97)$$

of the numbering used when the eigenvalues are real (10.90).

We define for all t in $[0, 1]$ the functions

$$\tilde{v}_{1,j}(t) = |v_{1,j}| \exp[it \arg(v_{1,j})], \quad (10.98)$$

where $\arg(v_{1,j})$ is the phase of the complex number $v_{1,j}$, $v_1 = \varepsilon_1, \mu_1$ and $j = 1, 2, \dots, J$. Substituting the numbers $v_{1,j}$ (where $v_1 = \varepsilon_1, \mu_1$) for $\tilde{v}_{1,j}(t)$ in equations (10.77,10.78), we obtain the matrix $\tilde{T}_1(\Lambda, t)$. For each value of t , we define the numbers $\tilde{\Lambda}_{n_1}^{(1)}(t)$ which satisfy

$$\text{tr} \tilde{T}_1 [\tilde{\Lambda}_{n_1}^{(1)}(t), t] - 2 \cos[k_1 d] = 0. \quad (10.99)$$

Then, the numbers $\tilde{\Lambda}_{n_1}^{(1)}(1)$ are the desired complex eigenvalues $\Lambda_{p_1}^{(1)}$ and the numbers $\tilde{\Lambda}_{n_1}^{(1)}(0)$ are real eigenvalues which can be determined using the method presented in the previous section 10.7.2. Assuming that $\tilde{\Lambda}_{n_1}^{(1)}(t)$ are continuous and differentiable functions of t , the complex numbers $\tilde{\Lambda}_{n_1}^{(1)}(1)$ can be estimated from the numbers $\tilde{\Lambda}_{n_1}^{(1)}(0)$ by a numerical integration [7] of

$$\frac{d\tilde{\Lambda}_{n_1}^{(1)}}{dt}(t) = - \frac{\text{tr}(\partial \tilde{T}_1 / \partial \Lambda) [\tilde{\Lambda}_{n_1}^{(1)}(t), t]}{\text{tr}(\partial \tilde{T}_1 / \partial t) [\tilde{\Lambda}_{n_1}^{(1)}(t), t]}, \quad (10.100)$$

where $\partial \tilde{T}_1 / \partial \Lambda$ is given by substituting the numbers $v_{1,j}$ for $\tilde{v}_{1,j}(t)$ in equations (10.94,10.93) and $\partial \tilde{T}_1 / \partial t$ is determined similarly. Finally the obtained estimates of numbers $\tilde{\Lambda}_{n_1}^{(1)}(1)$ are used to initiate any of the classical methods for the numerical solution of equations [7]. Then, one obtains the desired complex eigenvalues.

In order to eliminate the numerical instabilities, one has to multiply each matrix $T_{1,j}$ and their derivatives by the numbers N_j (10.95) as in the previous section 10.7.2.

10.7.4 Eigenfunctions

From (10.84), the expression of each eigenfunction $\phi_{n_1}^{(1)}$ is given by the coefficients of the column vectors $F_{n_1}(x_{1,j})$, $j = 0, 1, \dots, J$. On the numerical side, the only difficulty comes from the fact that numerical instabilities in the expression of the transfer matrices (10.78,10.79). A solution based on the R -matrix algorithm (or S -matrix) should consist in using the algorithm presented in [20] to obtain the vector $F_{n_1}(x_{1,0})$ (and the vector $F_{n_1}(x_{1,J}) = \exp[k_1 d] F_{n_1}(x_{1,0})$) and then, the algorithm presented in [21, section V] to obtain the vectors $F_{n_1}(x_{1,j})$, $j = 1, 2, \dots, J-1$. However, we propose to use another solution which benefits of the fact that we deal with 2×2 matrices.

We define the following complex coefficients:

$$\begin{bmatrix} \mathcal{F}_{11}^j & \mathcal{F}_{12}^j \\ \mathcal{F}_{21}^j & \mathcal{F}_{22}^j \end{bmatrix} = T_{1,J}(\Lambda_{n_1}^{(1)}) T_{1,J-1}(\Lambda_{n_1}^{(1)}) \cdots T_{1,j}(\Lambda_{n_1}^{(1)}), \quad (10.101)$$

$$\begin{bmatrix} \tau_{11}^j & \tau_{12}^j \\ \tau_{21}^j & \tau_{22}^j \end{bmatrix} = T_{1,j}(\Lambda_{n_1}^{(1)}) T_{1,j-1}(\Lambda_{n_1}^{(1)}) \cdots T_{1,1}(\Lambda_{n_1}^{(1)}), \quad (10.102)$$

$$\begin{bmatrix} \mathcal{F}_1^j \\ \mathcal{F}_2^j \end{bmatrix} = F_{n_1}(x_{1,j}) \quad j = 0, 1, \dots, J. \quad (10.103)$$

Since $F_{n_1}(x_{1,0})$ is an eigenvector of the matrix $T_1(\Lambda_{n_1}^{(1)})$ associated with the eigenvalue $\exp[k_1 d]$, its coefficients satisfy

$$\mathcal{F}_2^0 = -\frac{\mathcal{T}_{11}^J N - \exp[k_1 d] N}{\mathcal{T}_{12}^J N} \mathcal{F}_1^0, \quad (10.104)$$

where the numbers $\mathcal{T}_{11}^J N$ and $\mathcal{T}_{12}^J N$ are obtained by multiplying each coefficient of matrices $T_{1,j}(\Lambda_{n_1}^{(1)})$ by the number N_j . The coefficients \mathcal{F}_1^J and \mathcal{F}_2^J are deduced from (10.81,10.104) and then, one can obtain the other coefficients for $j = 1, 2, \dots, J-1$:

$$\begin{aligned} \mathcal{F}_1^j &= \frac{\mathcal{T}_{22}^{j+1} \tau_{11}^j N}{\mathcal{T}_{21}^{j+1} \tau_{11}^j N + \tau_{21}^j \mathcal{T}_{22}^{j+1} N} \left(\frac{\mathcal{F}_2^J}{\mathcal{T}_{22}^{j+1}} - \frac{\mathcal{F}_2^0}{\tau_{11}^j} \right), \\ \mathcal{F}_2^j &= \frac{\mathcal{T}_{11}^{j+1} \tau_{22}^j N}{\mathcal{T}_{11}^{j+1} \tau_{12}^j N + \tau_{22}^j \mathcal{T}_{12}^{j+1} N} \left(\frac{\mathcal{F}_1^J}{\mathcal{T}_{11}^{j+1}} - \frac{\mathcal{F}_1^0}{\tau_{22}^j} \right), \end{aligned} \quad (10.105)$$

where, as in (10.104), the multiplication by the number N consists in multiplying each coefficient of matrices $T_{1,j}(\Lambda_{n_1}^{(1)})$ by the number N_j .

Finally these functions have to be normalized. From the definition (10.89) of the inner product, one has to compute

$$\|\phi_{n_1}^{(1)}\|_{v_1}^2 = \frac{1}{d} \int_0^d |\phi_{n_1}^{(1)}(x_1)|^2 v_1(x_1) dx_1 \quad (10.106)$$

when the functions ε_1 and μ_1 have the property (10.88). In the general case (where ε and μ are complex valued functions), one has to use the formalism presented in [8, section 2.3]. It is possible to compute analytically the expression (10.106):

$$\begin{aligned} \|\phi_{n_1}^{(1)}\|_{v_1}^2 &= \frac{1}{2d} \sum_{j=1}^J \frac{w_{1,j}}{v_{1,j}} \left(|\mathcal{F}_1^{j-1}|^2 + \beta_{1,j}^{-2} v_{1,j}^{-2} |\mathcal{F}_2^{j-1}|^2 \right) \\ &\quad - \beta_{1,j}^{-2} \operatorname{Re} \left(i \overline{\mathcal{F}_1^{j-1}} \mathcal{F}_2^{j-1} - i \overline{\mathcal{F}_1^j} \mathcal{F}_2^j \right). \end{aligned} \quad (10.107)$$

This expression allows to eliminate the numerical instabilities which can occur from the exponential functions. Note that all the coefficients of matrices defined in sections 10.4 and 10.5 (matrices U , V and W) can be also computed analytically in order to eliminate the numerical instabilities.

References:

- [1] M. G. Moharam and T. K. Gaylord, "Rigorous coupled-waves analysis of metallic surface-relief grating," *J. Opt. Soc. Am. A* **3**, 1780–1787 (1986).
- [2] L. Li, "New formulation of the Fourier modal method for crossed surface-relief gratings," *J. Opt. Soc. Am. A* **14**, 2758–2767 (1997).
- [3] L. Li, "Justification of matrix truncation in the modal methods of diffraction gratings," *J. Opt. A: Pure Appl. Opt.* **1**, 531–536 (1999).
- [4] L. C. Botten, M. S. Craig, R. C. McPhedran, J. L. Adams, and J. R. Andrewartha, "The dielectric lamellar diffraction grating," *Optica acta* **28**, 413–428 (1981).
- [5] L. C. Botten, M. S. Craig, R. C. McPhedran, J. L. Adams, and J. R. Andrewartha, "The finitely conducting lamellar diffraction grating," *Optica acta* **28**, 1087–1102 (1981).
- [6] L. C. Botten, M. S. Craig, and R. C. McPhedran, "Highly conducting lamellar diffraction grating," *Optica acta* **28**, 1103–1106 (1981).
- [7] G. Tayeb and R. Petit, "On the numerical study of deep conducting lamellar diffraction grating," *Optica Acta* **31**, 1361–1365 (1984).
- [8] L. Li, "A modal analysis of lamellar diffraction gratings in conical mountings," *Journal of Modern Optics* **40**, 553–573 (1993).
- [9] B. Gralak, M. de Dood, G. Tayeb, S. Enoch, and D. Maystre, "Theoretical study of photonic band gaps in woodpile crystals," *Phys. Rev. E* **67**, 066 601 (2003).
- [10] E. Silberstein, P. Lalanne, J.-P. Hugonin, and Q. Cao, "Use of grating theories in integrated optics," *J. Opt. Soc. Am. B* **18**, 2865 (2001).
- [11] B. Gralak, R. Pierre, G. Tayeb, and S. Enoch, "Solutions of Maxwell's equations in presence of lamellar gratings including infinitely conducting metal," *J. Opt. Soc. Am. A* **25**, 3099 (2008).
- [12] A. Tip, A. Moroz, and J. M. Combes, "Band structure of absorptive photonic crystals," *J. Phys. A: Math. Gen.* **33**, 6223–6252 (2000).
- [13] B. Gralak and S. Guenneau, "Transfer matrix method for point sources radiating in classes of negative refractive index materials with $2n$ -fold antisymmetry," *Waves in Random and Complex Media* **17**, 581 (2007).

- [14] L. Li, “Formulation and comparison of two recursive matrix algorithms for modeling layered diffraction gratings,” *J. Opt. Soc. Am. A* **13**, 1024–1035 (1996).
- [15] L. Li, “Use of Fourier series in the analysis of discontinuous periodic structures,” *J. Opt. Soc. Am. A* **13**, 1870–1876 (1996).
- [16] M. Reed and B. Simon, Methods of Modern Mathematical Physics, Vol. IV: Analysis of Operators (Academic Press, 1978).
- [17] A. Figotin and V. Gorenstveig, “Localized electromagnetic waves in a layered periodic dielectric medium with a defect,” *Phys. Rev. B* **58**, 180–188 (1998).
- [18] D. Felbacq, B. Guizal, and F. Zolla, “Wave propagation in one-dimensional photonic crystals,” *Optics Communications* **152**, 119–126 (1998).
- [19] S.-E. Sandström, G. Tayeb, and R. Petit, “Lossy multistep lamellar gratings in conical diffraction mountings: an exact eigenfunction solution,” *Journal of Electromagnetic Waves and Applications* **7**, 631–649 (1993).
- [20] B. Gralak, S. Enoch, and G. Tayeb, “From scattering or impedance matrices to Bloch modes of photonic crystals,” *J. Opt. Soc. Am. A* **19**, 1547–1554 (2002).
- [21] D. M. Whittaker and I. S. Culshaw, “Scattering-matrix treatment of patterned multilayer photonic structures,” *Phys. Rev. B* **60**, 2610–2618 (1999).